Materials Science and Engineering A 527 (2009) 317–321

Contents lists available at ScienceDirect

Materials Science and Engineering A

journal homepage: www.elsevier.com/locate/msea

Effect of initial grain size on the joint properties of friction stir welded aluminum

Yufeng Sun [a], Hidetoshi Fujii [a,*], Yutaka Takada [a], Nobuhiro Tsuji [b], Kazuhiro Nakata [a], Kiyoshi Nogi [a]

[a] Joining and Welding Research institute, Osaka University, Ibaraki 567-0047, Japan
[b] Department of Materials Science and Engineering, Graduate School of Engineering, Kyoto University, Kyoto 606-8501, Japan

ARTICLE INFO

Article history:
Received 21 July 2009
Received in revised form 30 July 2009
Accepted 31 July 2009

Keywords:
Friction stir welding
Accumulative roll bonding
Ultrafine grained structure
Vickers hardness

ABSTRACT

In this study, 2 mm-thick commercial 1050-Al plates with an ultrafine grained (UFG) structure were obtained by the accumulative roll bonding (ARB) technique after a 5 cycle process and were subsequently joined by friction stir welding (FSW) at various revolution pitches (welding speed/rotation speed) of 1 mm/r, 1.67 mm/r and 2.5 mm/r. To understand the effect of the initial grain size on the welding properties, ARB processed samples followed by annealing under H24 conditions as well as the as-received samples in the fully annealed state were also applied to the FSW process. The microstructure evolution and Vickers hardness in the stir zone of all the samples were investigated. It was revealed that the annealed samples with an intermediate grain size finally obtained the most refined grain size and highest value of Vickers hardness in the stir zone. However, for the UFG samples, significant grain growth and corresponding decrease in hardness can be found in the stir zone.

1. Introduction

Friction stir welding (FSW), which is regarded as a solid-state welding process, was invented by TWI in 1991 in an attempt to weld aluminum alloys [1]. This joining technique is energy efficient, environment friendly and versatile. Up to now, many kinds of aluminum alloys from commercial pure aluminum to highly alloyed 2XXX and 7XXX series, which are generally considered as non-weldable, have been successfully joined by FSW technique. Nowadays, the application of FSW has been widely extended to a variety of materials including steel, copper, titanium alloys or even polymers [2–4]. However, because most FSW processed materials are conventional metals with grains usually larger than 1 μm, not much attention has been paid to the effects of grain size on the joint properties. Recently, with the rapid development of severe plastic deformation (SPD) technique, ultrafine grained (UFG) materials have attracted growing interest amongst material scientists. UFG materials have an average grain size of less than 1 μm and thus exhibit superior mechanical properties when compared with the coarse grained counterpart [5–9]. For example, 6 cycle accumulative roll bonded (ARB) pure aluminums show strength equivalent to low carbon steel [10]. There are many SPD techniques like ARB, ECAP and HPT to produce UFG metallic materials. However, due to some limitations of these SPD techniques such as the load capacity and frigidity of the equipment, the UFG materials still cannot be made large enough for industrial applications. Therefore, the welding or joining of UFG materials to produce a larger size has become very important. Obviously, the UFG material cannot be welded by the commonly used fusion welding, since the molten pool generated during the welding will inevitably destroy the UFG structure and result in a much coarser grain size in the solidified butt. Comparatively, FSW seems to be a very promising method for the joining of metallic materials with UFG structure. However, since the high heat generated by the friction between the rotation tool and the workpiece will inevitably lead to a temperature rise, it might bring the risk of recrystallization and coarsening of the UFG materials. Therefore, the size effect on the joint properties seems to be very important. Previously, Sato et al. and Topic et al. compared the hardness distribution in the stir zone of the ECAP and ARB processed aluminum with their coarse counterpart and found that hardness decrease did take place in the FSW processed materials with the UFG structure due to the coarsening of grain size [11–14]. Fujii et al. also observed the same phenomena in the ARB processed IF steel [15,16].

In this study, 2 mm-thick commercial 1050-Al plates with an ultrafine grained structure were obtained by the 5 cycle ARB process. The UFG plates were then FSW processed at various revolution pitches (welding speed/rotation speed). For comparison, an as-received sample with coarse grains and ARB followed by H24 annealed samples with an intermediate grain size were also FSW processed under the same conditions. The microstructure evolution and mechanical properties of these three kinds of samples with different initial grain sizes after the FSW process were investigated and the mechanism of the initial grain size dominated welding properties is discussed.

* Corresponding author. Tel.: +81 6 68798663; fax: +81 6 68798663.
E-mail address: fujii@jwri.osaka-u.ac.jp (H. Fujii).

0921-5093/$ – see front matter © 2009 Elsevier B.V. All rights reserved.
doi:10.1016/j.msea.2009.07.071

2. Experimental procedure

As-received commercial purity 1050-Al plates in the fully annealed state were used in this study as the starting materials. The UFG samples were obtained by the 5 cycle ARB process of the as-received plates. The details of the ARB process are described in refs [17,18]. To understand the size effect of the original materials on the microstructural evolution and mechanical properties of the FSW counterpart, some of the ARB samples were annealed under the H24 condition to obtain coarsened grains. However, the grain size of the annealed samples is still much less than that of the as-received sample. These three kinds of materials with different initial grain sizes, that is, the as-ARB samples, the ARB + annealed samples, together with the as-received samples, were then butt-welded along the rolling direction (RD) using an FSW machine. The samples used in the FSW process were 2 mm thick plates with 300 mm in length and 30 mm in width. In every FSW batch, two sample plates were put together and then FSW was processed parallel with the rolling direction. During the welding process, tools made of SKD61 were used and titled by 3°, which had a 12 mm-dia shoulder, 4 mm-dia probe and 1.8 mm probe height. The traveling speed was 1000 mm/min. Various rotation speeds, namely 400 rpm, 600 rpm and 1000 rpm, were used to evaluate the welding properties, which corresponds to the different revolution pitches of 1 mm/r, 1.67 mm/r and 2.5 mm/r, respectively. During the entire welding process, the temperature variations at the welding center were monitored using a thermocouple fixed at the bottom surface of the workpieces.

Following the welding processes, the Vickers hardness was measured on the centerline of the cross-section perpendicular to the welding direction. The microstructures of the welded samples were characterized by transmission electron microscopy (TEM) and the electron back-scattering diffraction (EBSD) technique. Thin foils perpendicular to the transverse direction (TD) and parallel to the welding direction were cut from the center of the weld for TEM observations and the planes parallel to the TD were cut from the weld for EBSD measurements. The cut specimens were then twin-jet electropolished in a mixed solution of HNO_3:CH_3OH = 3:7. The EBSD measurements were carried out using a program developed by TSL (OIM-Analysis 3.0 v) in a Philips XL30 SEM equipped with a field emission (FE) gun operated at 15 kV. The TEM observations were performed using a Hitachi H800 TEM operated at 200 kV.

3. Experimental results

Fig. 1 shows the EBSD maps showing the crystallographic orientations of these three kinds of samples, namely the as-received (a), ARB processed (b) and ARB + annealed samples (c). All the maps were observed from the TD. In these maps, only high-angle boundaries with misorientations higher than 15° were indicated by black lines. It can be seen that these three kinds of samples exhibit quite different microstructures and different mean grain sizes. The as-received sample has a fully annealed feature of equiaxial grains with the average grain size of about 13.1 μm, and no subgrains or dislocations are observed inside the grains. The ARB processed sample showed an ultrafine lamellar structure with the mean boundary interval less than 1 μm. Significantly elongated grains with lengths ranging from 2 μm to 10 μm were observed parallel to the TD. However, for the annealed samples, grain growth can be easily found in the EBSD map and the originally elongated grains become larger and somewhat equiaxial. But the lamellar structure was remained with a thicker boundary interval. The mean grain size of the annealed sample is about 8.4 μm, which lies between that of the as-received samples and the as-ARB processed sample.

TEM observations were further conducted to reveal the detailed microstructures. Fig. 2 shows the typical TEM images of the as-ARB and ARB + annealed samples. It is not easy to obtain the global microstructure of the as-received sample under TEM observation, since the grain size is too big. For the as-ARB processed sample shown in Fig. 2a, the lamellar boundaries are quite straight along the rolling direction. The microstructure in the ARB processed sample was rather pancake-shaped ultrafine grains nearly free from dislocations inside presumably due to the recovery and short range of gain boundary migration. The lamellar structure is uniform throughout the entire sample and the mean interval of the lamellar boundary is about 600 nm. However, for the ARB + annealed samples shown in Fig. 2b, the pancake-shaped grains can hardly be discerned and most of the grains are equiaxial, but with a grain size larger than that of the as-ARB sample. Some dislocation can still be found inside some grains or aggregates at some of the grain boundaries.

These three kinds of samples with different grain sizes were then applied to the FSW process at various revolution pitches of 1 mm/r, 1.67 mm/r and 2.5 mm/r. Fig. 3 shows the thermal profiles measured at the back of the workpieces during the FSW process. Since the thermal conductivity of aluminum is high, the temper-

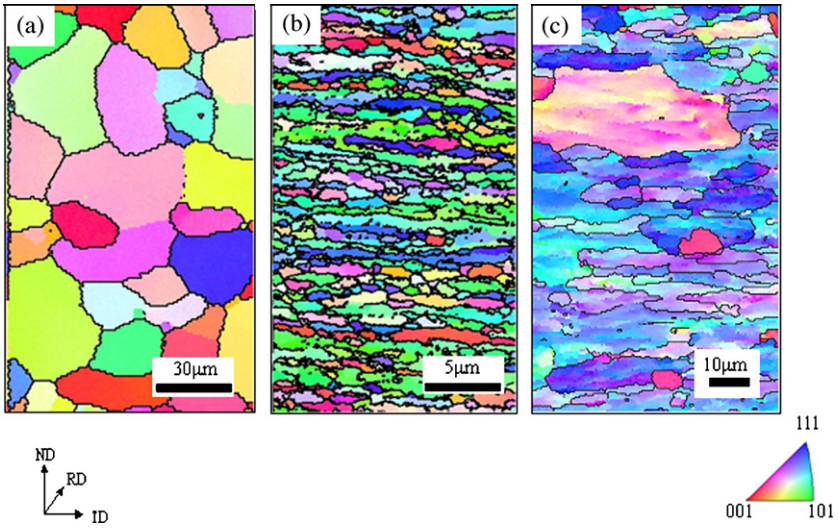

Fig. 1. EBSD map of 1050-Al with different grain sizes. (a) as-received; (b) ARB processed; (c) H24 annealed.

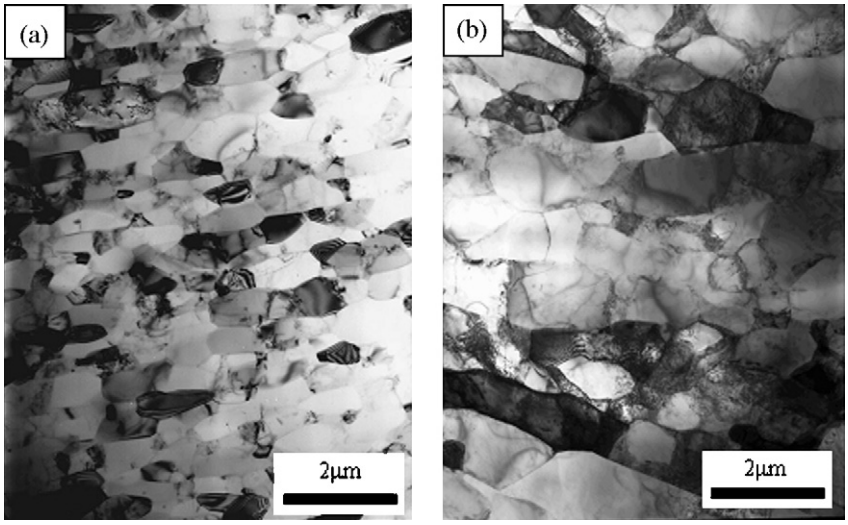

Fig. 2. TEM images showing the microstructure of (a) ARB processed and (b) ARB followed by H24 annealed 1050-Al.

ature rises sharply to its maximum value in 1 s when the rotating tools passed through the locations where the thermocouples were fixed in the workpiece. Then the temperature decreased gradually down to room temperature in less than 30 s. It was also found that the maximum temperature rise strongly depends on the revolution pitch. The higher the revolution pitch, the lower the temperature rise will be. The maximum temperature rise can reach to about 370 °C when the revolution pitch is 1.00 mm/r, and 300 °C when it is 1.67 mm/r.

The microstructures at the geometric center of the stir zone were characterized by EBSD. As a typical example, Fig. 4 shows the EBSD maps of the samples welding at a revolution pitch of 1.00 mm/r. The black lines in the figure separated the grains with grain boundary misorientations larger than 15°. For all the samples, only equiaxial grains can be found in the EBSP maps and color changes inside some grains surrounded by the black line, indicating the existence of subgrains or the pile-up of dislocations. The elongated grains in the ARB processed or the ARB + annealed samples cannot be found any more. Amongst the three kinds of samples welded at the same revolution pitch, the ARB + annealed exhibits the smallest grain size, although its original grain size falls between that of the as-received and as-ARB counterparts. It is worth mentioning that the grain size increases after the FSW process in the as-ARB processed sample. This phenomenon is quite unique since the usually refined structure can be obtained in the stir zone. When welded at higher revolution pitches of 1.67 mm/r and 2.5 mm/r, the same trend of microstructural evolution was observed. The average sizes of the grains with a high-angle boundary obtained from the EBSD maps of all three samples were summarized in Table 1. The grain sizes of all the FSW processed samples decrease with the increasing revolution pitch.

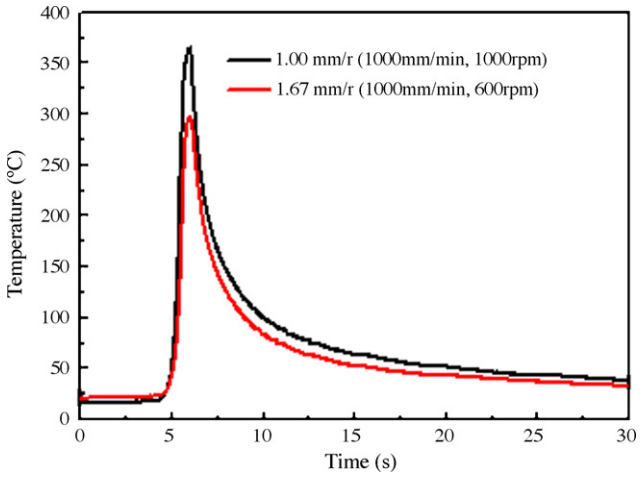

Fig. 3. Thermal profiles measured at the back of aluminum workpieces during FSW process with different revolution pitches.

Table 1
Grain size of the base materials and welded materials in the stir zone (μm).

Samples	Base material	Stir zone		
		1.00 mm/r	1.67 mm/r	2.50 mm/r
As-received	13.1	3.2	1.8	1.7
ARB + annealed	8.4	2.1	1.6	1.1
ARB	0.6	3.2	1.7	1.3

Fig. 5 shows the typical TEM bright field images of the stir zones in the as-received (a), the as-ARB (b) and the ARB + annealed samples (c). All of these three samples were welded at a revolution pitch of 1.67 mm/r. In the as-ARB processed sample, no pancake structure is observed. The microstructure reveals that all the samples consist of equiaxial grains with dislocations inside. However, the dislocation densities were not very high even after severe plastic deformation induced by the FSW. From the TEM observations, we found that after the FSW process the grain size of the annealed sample was smaller than those of the as-received sample and the ARB processed sample, which agrees well with the EBSD measurements.

Fig. 6 shows the horizontal hardness profile measured from the transverse cross-section of the three kinds of samples FS welded at the various revolution pitches. The as-received sample was not successfully FSW processed at a revolution pitch of 2.5 mm/r because its strength was not enough. It can be seen that for the as-received and ARB + annealed samples, the hardness in the stirred zone is higher than that in the base metals. While in the ARB processed sample, the FSW process resulted in an obvious reduction in hardness around the weld center. For example, the hardness in the stir zone of the ARB processed sample drops to 31 Hv from 46 Hv in the base metal when FSW processed at a revolution pitch of 1 mm/r. For all the samples, this hardness change spreads to about 5 mm away from the weld center on the centerline of the thickness of the plate, probably in the stir zone and TMAZ. As a result, the stir zone in the ARB + annealed samples shows higher hardness than those of the other two samples, which have a similar hardness in the stir zone

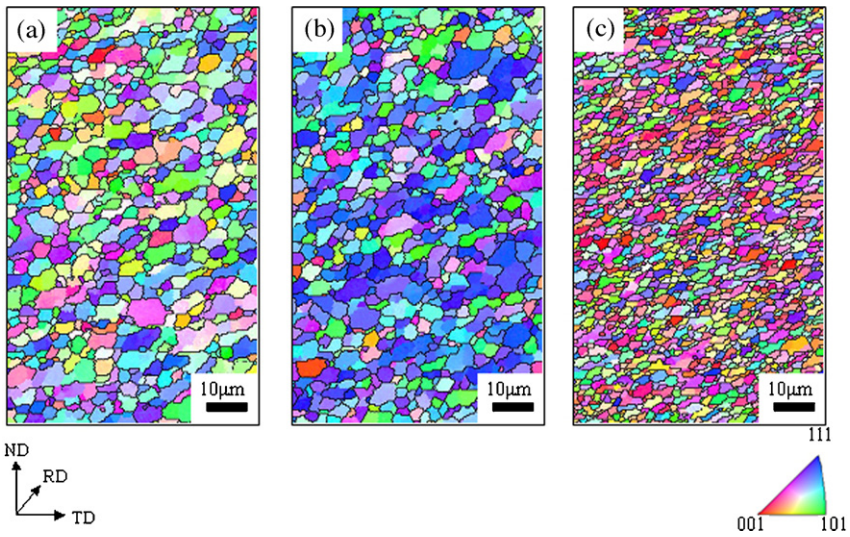

Fig. 4. EBSP maps showing the OIM in the stir zone of the FSW samples at a revolution pitch of 1 mm/r. (Observed from TD). (a) As-received; (b) as-ARB processed and (c) ARB + annealed samples.

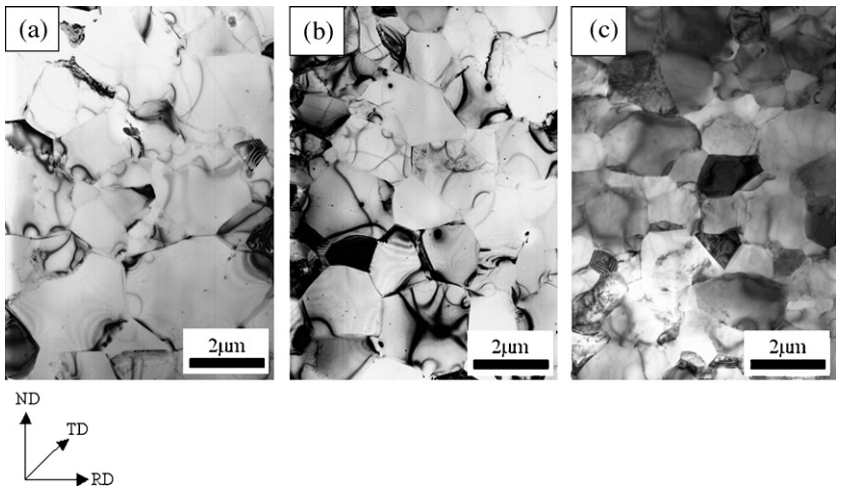

Fig. 5. TEM microstructures of stir zone welded at revolution pitch of 1.67 mm/r. (a) O aluminum (b) Ultrafine grained aluminum (c) ARB + annealed sample.

after the FSW process. Compared with the EBSD measurement, the Vickers hardness ordinarily increases with the decreasing grain size, which is in accordance with the classic Hall–Petch relationship. For the as-received and ARB + annealed samples, the hardness increase is larger when the revolution pitch is higher. Also, for the ARB processed samples, the hardness decrease is lower when the revolution pitch is higher.

4. Discussions

As we know, the evolution of the grain structure in the stir zone during the FSW may depends on the grain boundary structure, grain size and dislocation density of the initial microstructure. Usually, when the FSW technique is applied to conventional metals or alloys, the grain structure in the stir zone is formed by continuous dynamic recrystallization, which is characterized by a strain-induced progressive rotation of the subgrains with little boundary migration during the FSW process [12]. This process will eventually result in a significantly grain refinement and correspondingly higher strength in the stir zone than in the base material. However, when UFG materials like the ARB processed Al plates in the present study were FS welded, grain growth combined with a decrease in hardness were usually observed after the FSW process. Unlike conventional metals or alloys, a large quantity of vacancies or dislocations can be introduced into the as-ARB materials, which consist of pancake-shaped ultrafine grains mostly surrounded by high-angle boundaries. This kind of an ultrafine grained microstructure was found to be quite unstable upon thermal treatment, although it exhibits quite high strength [19]. That is, recovery can occur at relatively low temperatures to decrease the defect density within the grains. At the same time, continuous grain growth takes place and the mean grain size increases. At a lower temperature, the grain growth rate was relatively low and the grain boundary migration rate in both the directions parallel to the rolling direction and the direction perpendicular to the rolling direction were found to have a similar rate until the grains had reached equiaxial geometry. However, if the temperature is higher, i.e., from 200 °C to 250 °C for commercial purity Al, the grain growth becomes very rapid. In this study, the temperature rise in the FSW sample can reach 350 °C at the location where the rotating tools are passing through at a revolution pitch of 1 mm/r. Even at a revolution pitch of 2.5 mm/r, the temperature rise can reach above 250 °C. Therefore, it was proposed that the fragment of the ultrafine grains by the shear stress during the FSW process is not significant, while the rapid grain growth in the unstable microstructure will eventually result in coarse grains. For

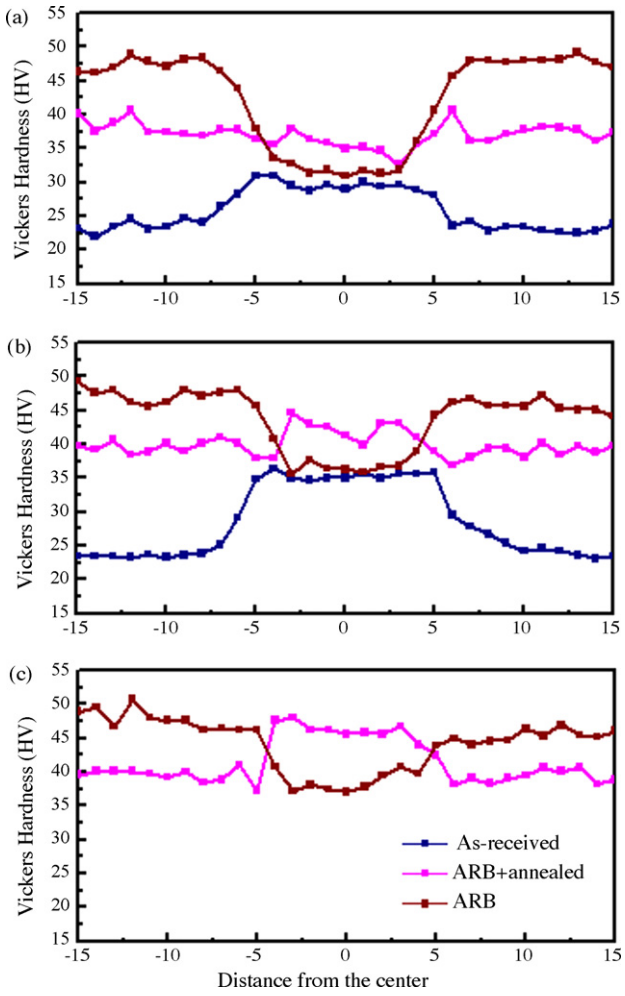

Fig. 6. Hardness profile of aluminum joints welded at revolution pitch of (a) 1 mm/r; (b) 1.67 mm/r and (c) 2.50 mm/r.

the as-received and ARB + annealed samples, the microstructure is relatively stable and the grain subdivision during the FSW process dominates rather than the grain growth caused by the temperature rise. As a result, a grain refinement was finally obtained.

5. Conclusions

In this paper, three kinds of 1050-Al alloy sheets with different initial grain sizes, namely, an ultrafine grained structure obtained by the ARB technique, an intermediate grain size obtained by annealing the ARB sample under the H24 condition, and the as-received materials in the fully annealed condition, were applied to the FSW process. The following conclusions can be drawn from the above experimental results.

The initial grain size exerts a significant influence on the microstructure in the stir zone of the FSW processed materials. The annealed sample with the intermediate grain size is the most preferable for obtaining the highest hardness in the stir zone with the smallest grain size.

After the FSW process, all the samples exhibit equiaxial grains in the stir zone despite of the initial grain shape or size of the materials.

The ultrafine grained structure of the ARB processed sample is unstable. The grain growth in the stir zone is believed to be caused by the temperature rise during the FSW process.

Acknowledgements

The authors wish to acknowledge the financial support of a Grant-in-Aid for Science Research from the Japan Society for Promotion of Science and Technology of Japan, the Global COE Programs, a Grant-in-Aid for the Cooperative Research Project of Nationwide Joint-Use Research Institute from the Ministry of Education, Sports, Culture, Science and Toray Science Foundation, ISIJ Research Promotion Grant, and Iketani Foundation.

References

[1] W.M. Thomas, E.D. Nicholas, J.C. Needham, International Patent Application No. PCT/GB92/02203, 1991.
[2] L. Cui, H. Fujii, N. Tsuji, K. Nogi, Scripta Mater. 56 (2007) 637–640.
[3] R. Nandan, T. Debroy, H.K.D.H. Bhadeshia, Prog. Mater. Sci. 53 (2008) 980–1023.
[4] Seth R. Strand, Ph.D thesis, Brigham Young University, 2004.
[5] R.Z. Valiev, R.K. Islamgaliev, I.V. Alexandrov, Prog. Mater. Sci. 45 (2000) 103–189.
[6] T.G. Langdon, Rev. Adv. Mater. Sci. 11 (2006) 34–40.
[7] S.H. Lee, Y. Saito, N. Tsuji, et al., Scripta Mater. 46 (2002) 281–285.
[8] N. Tsuji, Y. Saito, H. Utsunomiya, et al., Scripta Mater. 40 (1999) 795–800.
[9] N.Q. Chinh, P. Szommer, Z. Horita, T.G. Langdon, Adv. Mater. 18 (2006) 34–39.
[10] N. Tsuji, J. Nanosci. Nanotechnol. 7 (2007) 3765–3770.
[11] Y.S. Sato, M. Urata, H. Kokawa, K. Ikeda, M. Enomoto, Scripta Mater. 45 (2001) 109–114.
[12] Y.S. Sato, Y. Kurihara, S.H.C. Pack, H. Kokawa, N. Tsuji, Scripta Mater. 50 (2004) 57–60.
[13] I. Topic, H.W. Hoppel, M. Goken, Mater. Sci. Eng. A503 (2009) 163–166.
[14] I. Topic, H.W. Hoppel, M. Goken, Mater.Sci.Forum, 584–586(part 2) (2008) 833–839.
[15] H. Fujii, R. Ueji, Y. Takada, et al., Mater. Trans. 47 (2006) 239–242.
[16] H. Fujii, Y. Takada, N. Tsuji, K. Nogi, Proceedings of IIW pre-Assembly meeting on FSW in Nagoya, 2004, pp. 19–24.
[17] Y. Saito, H. Utsunomiya, N. Tsuji, T. Sakai, Acta Mater. 47 (1999) 579–583.
[18] N. Tsuji, Y. Saito, S.H. Lee, Y. Minamino, Adv. Eng. Mater. 5 (2003) 338–344.
[19] C. Kwan, Z.R. Wang, J. Mater. Sci. 43 (2008) 5045–5051.